J|A|C|S
ARTICLES
Published on Web 09/07/2002

Resolving the Different Dynamics of the Fluorine Sublattices in the Anionic Conductor $BaSnF_4$ by Using High-Resolution MAS NMR Techniques

Santanu Chaudhuri, Francis Wang, and Clare P. Grey*

Contribution from the Department of Chemistry, State University of New York, Stony Brook, New York 11794-3400

Received March 11, 2002

Abstract: ^{19}F and ^{119}Sn MAS NMR spectroscopy have been used to investigate the fluoride ion conductor, $BaSnF_4$, a member of the $MSnF_4$ family of fluorite-related anionic conductors containing double layers of Sn^{2+} and M^{2+} cations. Two fluorine sublattices were observed by ^{19}F MAS NMR, which could be assigned to specific sites in the lattice. The first sublattice is due to fluorine atoms located in Ba^{2+} double layers and is rigid on the MAS NMR time scale at room temperature. The second sublattice comprises the fluoride ions between the Ba^{2+} and Sn^{2+} layers, and the few fluorine atoms that inhabit the $Sn^{2+}-Sn^{2+}$ double layers. These ions are in rapid exchange with each other, and an extremely short correlation time τ_C for the motion of these ions of $<3 \times 10^{-5}$ s is obtained at -100 °C. T_1 measurements indicate that τ_C approaches 10^{-8} s at room temperature. ^{19}F-to-^{119}Sn cross-polarization (CP) experiments confirmed the assignments of the resonances, and that the fluorine atoms located next to the tin atoms are extremely mobile at room temperature (and thus do not contribute to the CP process). Two-dimensional ^{19}F exchange experiments showed that exchange between the rigid and mobile lattice does occur, but at a much slower rate ($\tau_C \approx 10$ ms at 250 °C). Low-temperature ^{19}F MAS and ^{19}F-to-^{119}Sn CP NMR spectra demonstrate that the motion of the fluoride ions has almost completely frozen out by -150 °C. The results are consistent with rapid two-dimensional (anisotropic) conductivity involving the fluoride ions between the Ba and Sn layers. Conductivity in three dimensions requires hops between the ions in the BaF_2-like layers and the mobile ions. This process does occur, but with exchange rates that are at least 6−7 orders of magnitude slower.

Introduction

$BaSnF_4$ is a member of the $MSnF_4$ (M = Pb, Ba, Sr) family[1,2] of layered anionic conductors, $PbSnF_4$ and its solid solutions showing the highest fluoride ion conductivities reported to date (10^{-3} Ω cm^{-1} at room temperature).[3] $PbSnF_4$ is of some technological interest because it can be used as an electrolyte in place of an oxide conductor in a solid-state oxygen sensor. Oxygen sensors containing oxide ion conductors such as yttrium-stabilized zirconia cannot be used below 500 °C, because the low oxide ion conduction at lower temperatures results in a very slow response of the cell to changes in the oxygen partial pressure.[4] In contrast, $PbSnF_4$-based amperometric sensors show greatly improved response times (25 s) at room temperature.[4−6] More recently, $PbSnF_4$ has also been used as an electrolyte and separator, allowing various metals, such as tungsten and vanadium, and C_{60} to be fluorinated under controlled conditions.[7]

At room temperature, $BaSnF_4$ and $SrSnF_4$ adopt a layered tetragonal (*P*4/*nmm*; $a = b = 4.3551$ Å and $c = 11.2323$ Å) structure, which is isostructural to the β-$PbSnF_4$ phase synthesized by using high-temperature methods. The $MSnF_4$ cation sublattice is derived from the fluorite structure, as adopted by β-PbF_2 and other MF_2 systems, but the cations are ordered forming alternating double layers of M and tin atoms along the *c*-direction of the tetragonal cell.[2,8−10] This cation ordering results in three different normal, fluorite-type sites for fluorine (Figure 1), i.e., between the two barium, the two tin, and the tin and barium layers. These will be referred to as the Ba−Ba, Sn−Sn, and Ba−Sn fluoride ions or the F3, F1, and F2, sites, respectively. Diffraction studies for the isostructural tetragonal phase of $PbSnF_4$ showed considerable disorder on the fluorine sublattice, particularly in the Pb−Sn and Sn−Sn layers.[2] The fluorine sites (F1's) in the Sn−Sn layers were found to be almost completely empty in a single-crystal study of an orthorhombic form of $PbSnF_4$, prepared hydrothermally.[11] In contrast, 28%

* Address correspondence to this author. E-mail: cgrey@sbchem.sunysb.edu.

(1) Pannetier, J.; Denes, G.; Lucas, J. *Mater. Res. Bull.* **1979**, *14*, 627−631.
(2) Denes, G.; Yu, Y. H.; Tyliszczac, T.; Hitchcock, A. P. *J. Solid State Chem.* **1991**, *91*, 1.
(3) Reau, J.-M.; Lucat, C.; Portier, J.; Hagenmuller, P.; Cot, L.; Vilminot, S. *Mater. Res. Bull.* **1978**, *13*, 877−882.
(4) Eguchi, T.; Kuwano, J. *Mater. Res. Bull.* **1995**, *30*, 1351−1357.
(5) Eguchi, T.; Suda, S.; Amasaki, H.; Kuwano, J.; Saito, Y. *Solid State Ionics* **1999**, *121*, 235−243.
(6) Kuwano, J.; Asano, M.; Shigehara, K.; Kato, M. *Solid State Ionics* **1990**, *40*, 472−475.
(7) Matuso, T.; Kakiya, T.; Sugie, Y. *J. Fluorine Chem.* **2000**, *101*, 257−261.
(8) Kanno, R.; Ohno, K.; Izumi, H.; Kawamoto, Y.; Kamiyama, T.; Asano, H.; Izumi, F. *Solid State Ionics* **1994**, *70*, 253−258.
(9) Ito, Y.; Mukoyama, T.; Funatomi, H.; Yoshikado, S.; Tanaka, T. *Solid State Ionics* **1994**, *67*, 301−305.
(10) Vilminot, S.; Perez, G.; Granier, W.; Cot, L. *Solid State Ionics* **1981**, *2*, 87−90.
(11) Chernov, S. V.; Moskvin, A. L.; Murin, I. V. *Solid State Ionics* **1991**, *47*, 71.

10.1021/ja026155j CCC: $22.00

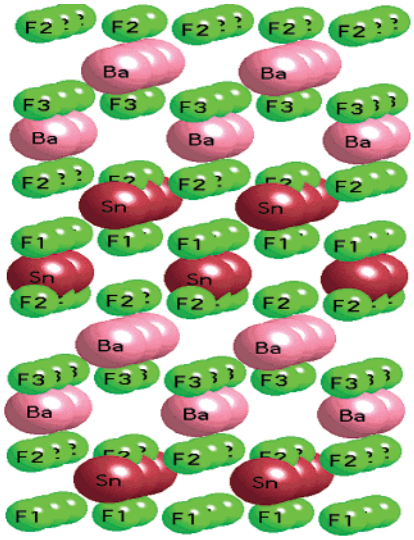

Figure 1. Layered structure of $BaSnF_4$ showing the cation double layers and three types of fluoride ions. The partially occupied F4 sites in the Ba−Sn layers have been omitted for clarity.

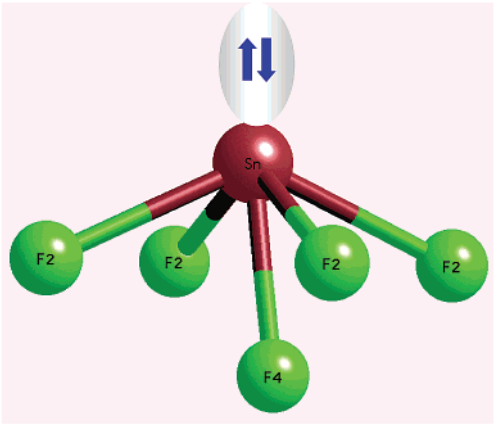

Figure 2. Sn coordination environment of $BaSnF_4$ (based on refs 2, 12, 13) showing the Sn(II) lone pairs pointing in the *c*-direction. Only one of the four partially occupied F4 sites in the Sn local coordination sphere is shown. Both the F2 and F4 sites are located in the Ba−Sn layers, while the Sn(II) lone pair is located in the Sn−Sn layer.

of these sites were occupied in a powder neutron diffraction study of β-$PbSnF_4$,[8] the displaced fluoride ions occupying a new site (F4) in the Pb−Sn layers (see Figure 2 for $BaSnF_4$).

To date, only an extremely brief report of a neutron diffraction study of $BaSnF_4$ has been published.[12] The tin environment, in this structure refinement, contains four F2 ions in its local coordination sphere, with four equal Sn−F bond lengths of 2.28 Å. Sn is also coordinated to four partially occupied F4 sites, with shorter bond lengths of 2.02 Å.[12] The four F4 sites, which are generated by the four-fold symmetry axis running through the tin atom, are very close together (>0.8 Å). Thus, only one site may be simultaneously occupied, consistent with the refined occupancy for this site (25%). This leads to an overall so-called SnF_5E-type coordination environment for Sn, E indicating the stereoactive lone pair of electrons on the tin(II) ion pointing in the *c*-direction (Figure 2). Mössbauer experiments have confirmed the pentacoordinated Sn(II) environments, while EXAFS studies of $PbSnF_4$ have shown that the local structure around the tin sites is less well defined than that around the lead sites.[2,12] The local environments of the F3 ions in the Ba−Ba layer are very similar to those in BaF_2-type environment.[13] However, the additional F4 ions in the Ba−Sn layers and the tetragonal distortion of the unit cell result in a slightly distorted cubic environment for the Ba^{2+} ions, with two sets of Ba−F bond distances: the Ba^{2+} ions are slightly shifted from the center of the F_8 cube, resulting in four slightly longer Ba−F2 bonds of 2.955 Å and four shorter Ba−F3 bonds (2.626 Å). In addition, the Ba^{2+} ions are coordinated to four more distant F4 ions at approximately 3.15 Å.

Although $BaSnF_4$ and $PbSnF_4$ are isostructural, $PbSnF_4$ is a so-called superionic conductor near room temperature, while $BaSnF_4$ shows between 1 and 2 orders of magnitude lower conductivity, the conductivities and activation energies for $BaSnF_4$ varying significantly in the two reported studies of this compound.[14,15] Fluoride ion conduction is thought to occur primarily in the M−Sn and Sn−Sn layers, and the size and polarizability of the M^{2+} cations appear to play a crucial role in controlling the conductivity and conduction mechanisms shown by these compounds. Wideline NMR reports have confirmed that there are two different sublattices with different mobilities.[15,16]

The diffraction studies provide only an average representation of the structure. Furthermore, the refinements of the structure of these relatively high symmetry materials were nontrivial, given the high level of disorder in these systems and the consequent problems with overlap of electron/neutron densities in the Fourier maps and the strong correlations between occupancies and thermal parameters. In addition, preferred orientation problems are often seen for powdered samples of layered materials.[2,8] Thus, the diffraction results do not necessarily provide a complete picture of the structure. Solid-state NMR may be used to probe local structure and is ideally suited to study the local environments and motion of the fluoride ions that are responsible for conduction in inherently disordered ionic conductors. For example, we have used ^{19}F MAS NMR to identify the anion sublattices responsible for motion in a series of fluorides, and to study the effect of cation doping on conduction mechanisms.[17−19] In more recent work, molecular dynamics (MD) studies were used to examine the effect of K^+ doping on the moderate ion conductor α-PbF_2 and to explore the predictions for the jump pathways made on the basis of our NMR experiments.[20] We have published preliminary results from a joint NMR and MD study of $BaSnF_4$ and $PbSnF_4$ in an earlier communication.[21] Here we present a detailed multinuclear NMR study of $BaSnF_4$. We chose to focus initially on $BaSnF_4$, because the time scales of the fluoride ion motion fall on the time scale probed by many high-resolution MAS NMR methods.

(12) Birchall, T.; Denes, G.; Ruebenbauer, K.; Pannetier, J. *Hyperfine Interact.* **1986**, *29*, 1331.
(13) Birchall, T.; Denes, G. *Can. J. Chem.* **1984**, *62* (3), 591−595.
(14) Denes, G.; Birchall, T.; Sayer, M.; Bell, M. F. *Solid State Ionics* **1984**, *8*, 213.
(15) Chadwick, A. V.; Hammam, E. S.; Van Der Putten, D.; Strange, J. H. *Cryst. Lattice Defects Amorphous Mater.* **1987**, *15* (1−4), 303−308.
(16) Floch-Durand, M. L.; Pannetier, J.; Denes, G. *Phys. Rev. B* **1986**, *33*, 632.
(17) Wang, F.; Grey, C. P. *J. Am. Chem. Soc.* **1995**, *117*, 6637.
(18) Wang, F.; Grey, C. P. *Chem. Mater.* **1997**, *9*, 1068.
(19) Wang, F.; Grey, C. P. *J. Am. Chem. Soc.* **1998**, *120*, 970.
(20) Castiglione, M. J.; Madden, P. A.; Wilson, M. *J. Phys.: Condens. Matter* **1999**, 9009.
(21) Chaudhuri, S.; Castiglione, M.; Wang, F.; Wilson, M.; Madden, P. A.; Grey, C. P. *Study of Fluoride Ion Motions in $PbSnF_4$ and $BaSnF_4$ Compounds With Molecular Dynamics Simulation and Solid State NMR Techniques*; Materials Research Society Proceedings, Solid State Chemistry of Inorganic Materials III, Boston, 2000; Materials Research Society: Warrendale, PA, 2002.

By using ^{19}F, ^{119}Sn, and $^{19}F/^{119}Sn$ NMR one-dimensional and two-dimensional (2D) experiments, we show that there are two distinct fluorine sublattices, which can be assigned to specific sites in the lattice. The fluoride ions between the Ba layers are held rigidly in the lattice and exchange only very slowly with the set of very mobile fluoride ions in the Ba−Sn and Sn−Sn layers. All the ions between the Ba−Sn and Sn−Sn layers are involved in the conduction process. This results in highly anisotropic motion in these layers, the Ba−Ba layers acting as barriers to three-dimensional conductivity. Motion in the Ba−Ba layers is proposed to occur primarily via jumps into the Ba−Sn sites and not directly between sites in the Ba−Ba layers.

Experimental Section

Materials Preparation. $BaSnF_4$ was prepared by the solid-state reaction of stoichiometrically equivalent amounts of BaF_2 and SnF_2. The metal fluorides were mixed thoroughly in an N_2 atmosphere by using an agate mortar. The powder was packed in a Cu tube, which was then crimped to minimize exposure to the outside air. The Cu tube was then placed in a quartz-glass tube and sealed under vacuum. The quartz tube was heated at 250 °C for 8 h, followed by 1 h at 500 °C, and slowly cooled to room temperature at 0.5 °C/min. No impurities were observed in the X-ray powder diffraction pattern of the resultant product, and the pattern matched the simulated powder pattern calculated using the reported cell parameters for $BaSnF_4$. Neutron diffraction experiments performed at ISIS (at the Rutherford Laboratory, UK) of a sample prepared using the same method, but on a much larger scale, did reveal the presence of small impurities that were not detected in the powder pattern obtained with the laboratory X-ray diffractometer. These included very small concentrations of BaF_2 and an as-yet unidentified third phase.

NMR. NMR experiments were performed on a 360 MHz Chemagnetics spectrometer with operating frequencies of 338.75 and 134.12 MHz for ^{19}F and ^{119}Sn, respectively. The NMR spectra were collected with a double-resonance Chemagnetics 4 mm pencil probe at spinning speeds of 12−19 kHz and with a 2 mm probe, built by A. Samoson and co-workers, that is capable of reaching MAS frequencies of 45 kHz.[22] ^{19}F and ^{119}Sn spectra were referenced to liquid $CFCl_3$ at 0 ppm and the secondary reference, solid SnO_2 at −604.3 ppm (when referenced to the primary reference $Sn(CH_3)_4$ at 0 ppm),[23] respectively. Standard one-pulse and rotor-synchronized Hahn-echo ($\pi/2-\tau-\pi-\tau-$acquire; τ = 1 rotor period) pulse sequences were employed for data acquisition. Two-dimensional magnetization exchange NMR spectroscopy was used to study the exchange between fluorine sites. Experiments were performed as a function of the rotor-synchronized mixing time interval (T_m) from 4 to 56 ms. A standard cross-polarization (CP) pulse sequence was used with a flip-back pulse on the ^{19}F spins following data acquisition.[24] Na_3SnF_6 was used as a standard to set the Hartmann−Hahn match under MAS conditions, and the match was optimized for a 12 kHz spinning speed. An inversion−recovery pulse sequence was employed to measure the spin−lattice relaxation times (T_1's) at different temperatures. The ^{19}F relaxation times in the rotating frame ($T_{1\rho}$'s) were measured by using a standard spin-locking pulse sequence by varying the spin-locking time. Typical recycle delays of 40 s for tin and 2 s for fluorine were used, along with $\pi/2$ values of 3.2 and 3.3 μs for ^{19}F and ^{119}Sn, respectively.

Nitrogen was used as both the spinning and purge gas for the variable-temperature experiments. The actual temperatures for the 4 mm probe at different spinning and temperature conditions were determined in a separate set of experiments by using the temperature dependence of the ^{207}Pb chemical shift of $Pb(NO_3)_2$. The actual temperatures at moderate spinning speeds >13 kHz are typically 10−15 °C higher than the measured temperatures, except for the low-temperature data (measured temperatures of between −150 and −130 °C), where the real temperatures are 20−30 °C higher. The measured temperatures are quoted in the text.

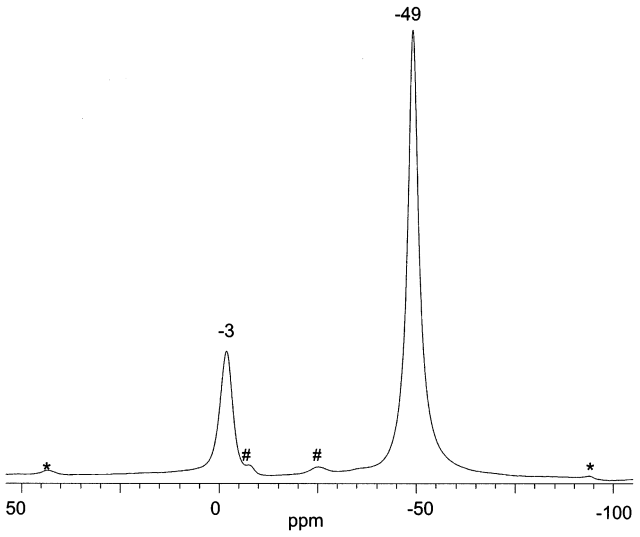

Figure 3. ^{19}F MAS NMR spectra of $BaSnF_4$ at a spinning speed (ν_r) of 19 kHz, showing the two different fluoride ion environments. The isotropic peaks are labeled. The ∗ and # denote the spinning sidebands of the −3 ppm peak and the impurity peaks, respectively.

Results

^{19}F and ^{119}Sn Variable-Temperature MAS NMR. The ^{19}F MAS NMR spectrum of $BaSnF_4$ (Figure 3) at room temperature shows two clearly resolved resonances at −3 and −49 ppm. Unlike the resonance at −3 ppm, the resonance at −49 ppm has a Lorentzian line shape and no associated spinning sidebands, suggesting that it is due to fluoride ions that are mobile on the time scale of the ^{19}F homonuclear coupling. This is consistent with earlier wideline ^{19}F NMR results for $BaSnF_4$, where two sublattices could be distinguished on the basis of their different dynamics.[15,16]

The two resonances can readily be assigned, given the chemical shifts for BaF_2 (−13.6 ppm) and SnF_2-type environments (−40 to −100 ppm in SnF_2[25,26]). The fluoride ions in the Ba−Ba layer (F3; Figure 1) have local environments that are very similar to that in BaF_2, and thus the −3 ppm resonance is assigned to ions in these layers. The resonance at −49 ppm is assigned to the remaining fluoride ions that are undergoing rapid chemical exchange between different sites in the Ba−Sn and Sn−Sn layers. The assignment is supported by the ratio of the peak areas calculated from the one-pulse ^{19}F NMR spectrum of 1:3.1 (±0.1) for the −3 and −49 ppm resonances, respectively, since there are 3 times more fluoride ions in a combination of the Ba−Sn and Sn−Sn layers than in the Ba−Ba layers. The small resonance at approximately −8 ppm is due to an impurity and is tentatively assigned to BaF_2 or Sn^{2+}-doped BaF_2 on the basis of our neutron diffraction results.

(22) Du, L.-S.; Samoson, A.; Tuherm, T.; Grey, C. P. *Chem. Mater.* **2000**, *12* (12), 3871−3878.
(23) Clayden, N. J.; Dobson, C. M.; Fern, A. *J. Chem. Soc., Dalton Trans.* **1989**, *5*, 843−847.
(24) Michel, D.; Engelke, F. *NMR Basic Principles Prog.* **1994**, *32*, 69.
(25) Wang, F. Probing the Disorder, Mobility and Defect Structure of Disordered Inorganic Fluorine Anionic Conductors by High-Resolution Solid State NMR. Ph.D. Thesis, SUNY Stony Brook, 1998.
(26) Le Floch-Durand, M.; Haerberlen, U.; Muller, C. *J. Phys.* **1982**, *43*, 107.

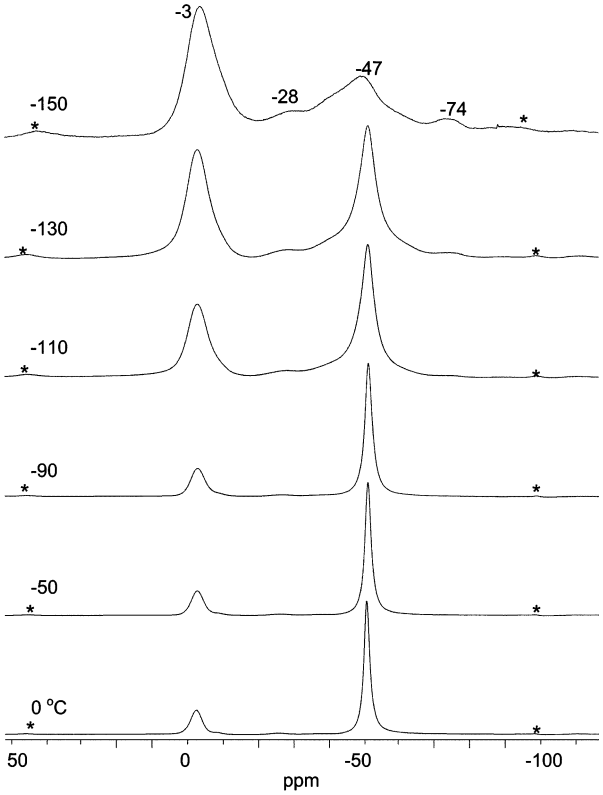

Figure 4. Low-temperature ^{19}F MAS NMR echo spectra ($\nu_r = 16$ kHz; 15.3 kHz at −150 °C) of $BaSnF_4$, showing the gradual slowing down of the fluoride ion motion as the temperature is lowered. The ∗'s indicate spinning sidebands.

^{19}F variable-temperature NMR experiments were performed to follow the chemical exchange between the different fluorine sublattices. A dramatic change in the echo spectra is seen (Figure 4) as the temperature is reduced from room temperature to −150 °C. A series of sites become visible as the ionic motion freezes out on the chemical shift time scale. The resonances also broaden considerably, and the intensity of the sidebands increases dramatically as the reduced motion of fluoride ions reintroduces the homonuclear ^{19}F dipolar coupling between all the fluoride ions. Additional broadening may also result from a distribution of local environments for fluorine, due to the disorder in the Ba−Sn and Sn−Sn layers. Analysis of the lowest temperature spectrum is complicated due to the overlap of the broad resonances and their spinning sidebands. Nonetheless, at least three new resonances at −28, −47, −74 ppm are resolved. On the basis of the chemical shifts of SnF_2, we tentatively assign the weaker −74 ppm resonance to the Sn−Sn layer fluoride ions. The broad resonances at −47 and −28 ppm are assigned to the disordered fluoride ion sites in the Ba−Sn layers. The apparent decrease in the relative intensity of the Ba−Ba resonance at −3 ppm is not believed to be real but is a consequence of the large fraction of the intensity contained in the sidebands for the broader −28, −47, and −74 ppm resonances, in combination with their shorter T_2's. Further confirmation of the validity of these suggestions is seen by comparing the one-pulse and the echo spectra, both acquired at −150 °C (shown in the Supporting Information, Figure S1), the relative intensity of the −3 ppm resonance decreasing in the one-pulse spectrum due to the longer T_2 associated with this resonance.

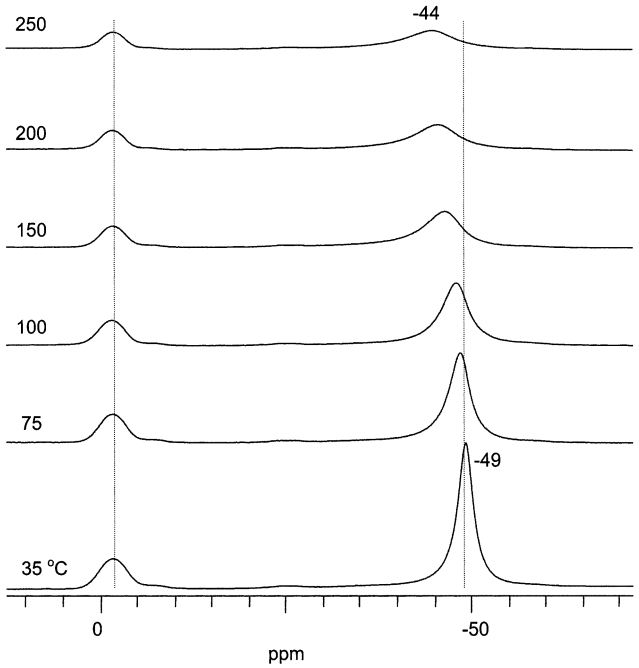

Figure 5. Enlargement of the ^{19}F MAS NMR spectra, showing the effect of temperature on the two $BaSnF_4$ isotropic resonances ($\nu_r = 17$ kHz), in the temperature range of 35−250 °C.

The observation of a single, motionally averaged resonance at −100 °C and above indicates that the fluorine ions in the Ba−Sn and Sn−Sn layers must be undergoing very rapid jumps between the different sites that give rise to the resonances at −28, −47, and −74 ppm with a rate, k (=$1/\tau_c$, where τ_c is the correlation time associated with the motion), that is greater than the frequency separation between these resonances. The correlation time required for coalescence, $\tau_{coal.}$, can be readily estimated[27] and is given by $2^{1/2}/\pi(\nu_A - \nu_B)$ (where $\nu_A - \nu_B$, the separation in hertz between the resonances, is ∼15 kHz); thus, the ions are moving with a rate that is greater than 3×10^4 s^{-1} at ≥−100 °C.

A small shift of the ^{19}F mobile, fluoride-ion resonance from −49 ppm at room temperature to −44 ppm at 250 °C is observed as the temperatures is raised, along with a broadening of this resonance (Figure 5). The shift indicates that the average fluorine environment changes with temperature. This implies that either the time spent by the mobile fluorine atoms in the different fluoride ion sites changes as a function of temperature, or new sites start to become occupied as the temperature increases. One possible explanation for this shift is that these new sites correspond to some of the F3 sites in Ba−Ba layers; i.e., the Ba−Ba fluoride ions become involved in the motion (on the time scale probed by this experiment, $\tau_C < 10^{-5}$ s) at higher temperatures. Exchange between the rigid and mobile sublattices, involving a single correlation time, should be accompanied by a broadening of the resonances from *both* sublattices. This is not observed experimentally. This broadening may not necessarily be seen (or may be difficult to detect) either for motion involving a distribution of correlation times or for motion involving only a subset of the Ba−Ba ions. To test this latter suggestion, we examined the intensities of the resonances as a function of temperature, to determine whether any

(27) Abragam, A. *The Principles of Nuclear Magnetism*; Oxford University Press: Oxford, 1961.

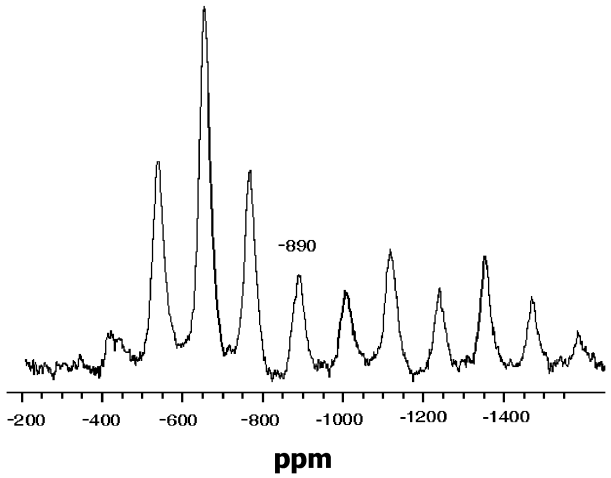

Figure 6. ^{119}Sn one-pulse MAS NMR spectrum ($\nu_r = 17$ kHz), showing the large spinning sideband manifolds and an isotropic resonance at −890 ppm.

significant changes in the populations of the sublattices could be detected. Both the −3 and −44 to −49 ppm resonances are predicted to lose 55% of their initial intensity when the temperature is increased from 35 to 250 °C, on the basis of a calculation of the normal Boltzman distributions for ^{19}F at a static magnetic field strength of 8.4 T. Integration of the peak area reveals that both sets of resonances drop by approximately 53(±5)%, and no significant change in the ratio of mobile to rigid resonances is observed, suggesting that the shift in the resonance is not associated with a significant depopulation of the Ba−Ba layers and rapid exchange between the two sublattices.

The room-temperature, one-pulse ^{119}Sn MAS NMR spectrum of $BaSnF_4$ shows large spinning sideband manifolds, consistent with a large chemical shift anisotropy (CSA) for the tin atoms (Figure 6). The sideband manifold was simulated using Herzfeld−Berger[28] methods to extract the three principal values, σ_{11}, σ_{22}, and σ_{33}, of the shielding tensor. The best fit to the experimental spectra was obtained with a span Ω ($=\sigma_{33} - \sigma_{11}$) of 890 ppm, a skew χ ($3(\delta_{22} - \delta_{iso})/\Omega$) of 1.0, and an isotropic chemical shift δ_{iso} of −893 ppm. A skew value of 1.0 indicates an axially symmetric shielding tensor. The large value of span ($\Omega = \sigma_{33} - \sigma_{11}$) is slightly smaller than the value obtained for SnO (975 ppm[29]) but much larger than that found in five-coordinate tin(IV) compounds such as K_2SnO_3 (367 ppm[23]), consistent with a highly distorted electron cloud surrounding the tin(II) atoms and the presence of a stereoactive lone pair.

The low-temperature ^{119}Sn spectra were slightly broader than those at room temperature, presumably due to a distribution of (rigid) fluorine positions in the tin local coordination sphere, and the CSA increased slightly.[25] The signal-to-noise ratio of the low-temperature ^{119}Sn MAS NMR spectra was not very high, since a very long acquisition period was required to achieve a good signal-to-noise ratio. Thus, we did not attempt to quantify the change in the CSA parameters with decreasing temperature.

Cross-Polarization Experiments and $T_{1\rho}$ Measurements. Cross-polarization experiments were performed to help confirm the assignments of the different ^{19}F resonances and to probe

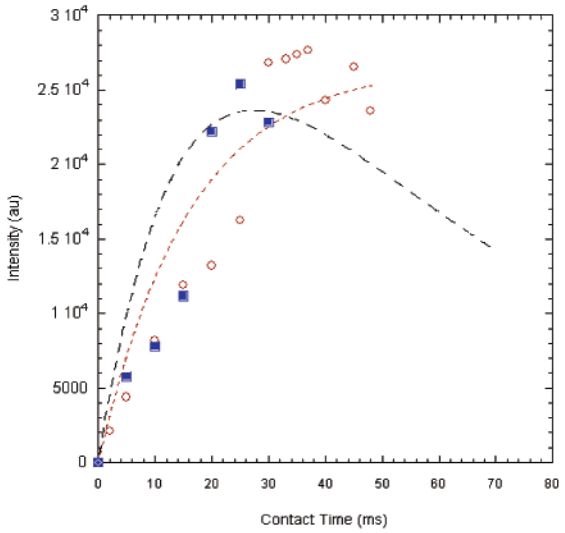

Figure 7. ^{19}F-to-^{119}Sn CP intensity, plotted as a function of the contact time. Two separate sets of data are plotted, which depend on the ^{19}F Larmor frequency used for the original $\pi/2$ pulse and the spin-locking. The filled squares and open circles represent on-resonance irradiation of the F_R and F_M fluoride ions, respectively. Two CP dynamics curves are shown. The first (− −) represents the best fit to the experimental data, obtained with a simple ($1 - \exp(-t/T_{IS})$) growth curve. The second (- -) is calculated, using the measured $T_{1\rho}$ value and the calculated value of T_{IS} (see text).

the dipolar couplings between the tin and fluorine sublattices. The relaxation times in the rotating frame (the $T_{1\rho}$ values) were first determined for the two ^{19}F sublattices, in view of the strong dependence of the CP efficiency on these values. The intensities of the two resonances were measured at room temperature with a spin-locking pulse sequence, as a function of the spin-locking time. Both sets of data could be fit to a single-exponential decay curve, yielding $T_{1\rho}$ values of 0.77 ± 0.03 and 52 ± 5 ms for the mobile and rigid fluoride sublattices, respectively. Thus, the mobile fluoride ions will remain spin-locked only for a very short period of time in comparison to the static fluoride ions.

Two sets of CP experiments were performed by setting the ^{19}F carrier frequency to the frequency of either the rigid sites (F_R) or the mobile (F_M) sites. In both sets of experiments, the ^{119}Sn magnetization grew very slowly with increasing contact time. Only very slightly different CP profiles (Figure 7) were obtained in these two experiments, the maximum ^{119}Sn magnetization being achieved at approximately 30 ms. ^{119}Sn magnetization dropped slightly between 35 and 50 ms. The initial part of the CP profile is, to a first approximation, independent of any $T_{1\rho}$ effects and may be used to estimate the polarization transfer time, T_{IS}. A fit to the first 20 ms of the CP profile (short-dashed line, Figure 7) yielded an approximate value for T_{IS} of 16 ms. (Fits to the first 5−10 ms of the data, which should be less affected by the $T_{1\rho}$ relaxation, resulted in an apparent increase in T_{IS} to 20 ms, the increase most likely reflecting errors in the measurements of the ^{119}Sn intensity.) Given the extremely short $T_{1\rho}$'s measured for the mobile fluoride ions (i.e., $(T_{1\rho})_M \ll T_{IS}$), the fluoride ions in the Ba−Ba layers must be primarily responsible for the polarization transfer. Furthermore, the relatively long T_{IS} value indicates that the fluoride ions in the tin first anion coordination sphere are not involved in the CP process. This provides further confirmation that (i) the resonance at −3 ppm is not due to fluorine directly coordinated to the tin, i.e., in the Sn−Sn or Ba−Sn layers, and (ii) the fluorine atoms near the tin ions are mobile.

(28) Herzfeld, J.; Berger, A. E. *J. Chem. Phys* **1980**, *73*, 6021−6030.
(29) Cossement, C.; Darville, J.; Gilles, J. M.; Nagy, J. B.; Fernandez, C.; Amoureux, J. P. *Magn. Reson. Chem.* **1992**, *30*, 263−270.

The CP efficiency is sensitive to the offset frequency of the ^{19}F radio frequency (rf) field,[30] the efficiency of the polarization transfer decreasing by Δ,

$$\Delta = 1 - \nu_1^2/(\nu_1^2 + \delta_{off}^2) \quad (1)$$

as the offset frequency (δ_{off}) of the applied rf field is increased. Given an rf field strength (ν_1) of 78 kHz and a maximum offset frequency of only 15 kHz (i.e., $\nu(F_R - F_M)$), the reduction in CP efficiency is small (<4%) for off-resonance ^{19}F irradiation of the F_R spins at the F_M frequency and will not be considered further.

The CP experiments were repeated at low temperatures (−150 °C) under conditions where the ionic motion should be considerably reduced, in an attempt to transfer polarization from *all* the sublattices. As before, the ^{19}F $T_{1\rho}$'s were measured initially at −150 °C to explore the spin-locking efficiency of the different sites. The intensities of the resonances at −3, −47, and −74 ppm were measured as a function of the spin-locking time (see Supporting Information, Figure S2). Due to overlap problems, the intensity of the resonance at −28 ppm could not be readily determined. Fits to the experimental data by using a single-exponential curve yielded very similar $T_{1\rho}$ values of 2−3 ms. The fits are not good, and the behavior is clearly more complex than this simple $T_{1\rho}$ analysis suggests. The important point to note, however, is the difference between the room- and low-temperature $T_{1\rho}$ values. The $T_{1\rho}$ values for the Ba−Ba-like environment have decreased from 41 to 2 ms, whereas the $T_{1\rho}$'s of the mobile fluoride ions have actually increased to 2−3.3 ms (from a room-temperature value of 0.7 ms). Presumably, the freezing out of the ionic motion at low temperatures on the $T_{1\rho}$ time scale, and the accompanying reintroduction of the homonuclear coupling between all the fluorine ions, results in a more strongly coupled spin bath with similar $T_{1\rho}$ values.

The short $T_{1\rho}$'s for all the sites resulted in very inefficient polarization transfer in the low-temperature CP experiment, and consequently, the signal-to-noise ratios of the ^{119}Sn spectra were very poor. The slightly larger ^{119}Sn CSA and broader isotropic resonance may also contribute to the poorer CP efficiency at low temperatures. On the basis of data collected with spin-locking times of 0.5, 1, and 2 ms (with the ^{19}F carrier frequency set at a frequency intermediate between those of the F_R and F_M sites), a maximum in the tin magnetization was observed between 1 and 2 ms. This suggests that T_{IS} has decreased significantly at lower temperatures.

Calculations of the Polarization Transfer Rates. To compare the experimentally determined values of T_{IS} with those calculated for the $BaSnF_4$, we require a model with which to describe the spin system, which should *ideally* be able to account for the mobility of a subset of the fluoride ions. The simplest approach, and one that has been widely used to analyze the CP dynamics in extended, nonrotating solids, is based on a calculation of the Van Vleck second moments ($M_{2(II)}$ and $M_{2(IS)}$) that describe the homonuclear and heteronuclear couplings.[24,30] The method is expected to work well under conditions of strong I−I homonuclear couplings and slow to moderate magic angle spinning. The second moments may be readily calculated for a solid by using the following expressions:[31]

$$M_{2(II)} = \frac{3}{5}\left(\frac{\mu_0}{4\pi}\right)^2 \gamma_1^4 \hbar^2 I(I+1) \sum_j \frac{1}{r_{ij}^6} \quad (1)$$

$$M_{2(IS)} = \frac{4}{15}\left(\frac{\mu_0}{4\pi}\right)^2 \gamma_S^2 \gamma_I^2 \hbar^2 S(S+1) \sum_k \frac{1}{r_{ik}^6} \quad (3)$$

where the individual terms are expressed in terms of gyromagnetic ratio and the distance between the spins (r_{ij}). Due to the $(1/r_{ij})^6$ dependence of the second moment, the calculation converges quickly, even in an extended solid. T_{IS} can then be expressed[32] in terms of Van Vleck second moments:

$$\frac{1}{T_{IS}} = \frac{3}{2} M_{2(IS)} \left(\frac{2\pi}{5 M_{2(II)}}\right)^{1/2}$$

The rate of polarization transfer between two (I and S) coupled spin-$^1/_2$ spin reservoirs can be described by a cross-polarization transfer rate, $1/T_{IS}$. The buildup in S magnetization, $\beta_s(t)$ (assumed to be zero at $t = 0$), can be described by the following equation, assuming a single rate process:[30]

$$\beta_s(t) = -\frac{1}{1-\lambda}(1 - e^{-(1-\lambda)t/T_{IS}})\, e^{-t/T_{1\rho}}\, \beta_{I0} \quad (5)$$

and $\lambda = T_{IS}/T_{1\rho}(^{19}F)$. β_{I0} represents the initial I-spin magnetization. This expression assumes that the $T_{1\rho}$ values for the S spins are much longer than those of the I spins and that the S spins are dilute.

Under the relatively fast MAS conditions used in the work described in this paper, and the fairly weak homonuclear coupling (in comparison to many proton-containing systems), the approach is not expected to be completely valid at room temperature and above. A numerical calculation, using the full Hamiltonian, is, however, nontrivial given the large number of spins that would be required to produce a realistic spin system. Other methods, which involve modification of the thermodynamic approach described above, also require additional assumptions and are also suitable only under slow or moderate MAS conditions. Thus, we have used the simple second moment (i.e., thermodynamic) approach to provide an approximate of T_{IS}, but we recognize that there are limitations of this method, especially for our systems, which may result in calculated T_{IS} values that are shorter than those observed experimentally.

Equations 2 and 3 were used to calculate the homonuclear and heteronuclear second moments, to compare the theoretical cross-polarization rate ($1/T_{IS}$) with the experimental data. We have used two models to describe the fluorine spin bath and predict the effect of motion on the CP dynamics. In the first model (the model for the rigid solid), we assumed that all the fluoride spins contribute to the polarization transfer, while in the second model (the model for one rigid and one mobile sublattice), the rapidly moving fluoride atoms in the Ba−Sn and Sn−Sn layers (with short $T_{1\rho}$ values) were not assumed to contribute to the polarization transfer.

Model I. The second moments have been calculated for the rigid solid by including all the ^{19}F spins within a sphere of 8 Å

(30) Mehring, M. *Principles of High-Resolution NMR in Solids*; Springer: Berlin-Heidelberg-New York, 1983.
(31) Vleck, J. H. V. *Phys. Rev* **1948**, *74*, 1168.
(32) Michel, D.; Engelke, F. Cross-polarization, Relaxation Times and Spin-diffusion in Rotating Solids. In *Solid State NMR III: Organic Matter*; Dehl, P., Fluck, E., Gunther, H., Kosfeld, K., Seelig, J., Eds.; Springer-Verlag: Berlin, 1994; Vol. 32, p 69.

radius from a central atom (Sn or F). To account for the presence of partially occupied F4 sites, the calculations were performed by assuming that only one of the four nearby sites was occupied (i.e., the Sn is coordinated to four F2's and one F4 site only). To simplify the calculation further, we placed a single F4 atom on the center of the square formed by the four possible F4 positions obtained in the neutron diffraction study (see Figure 2)[8,12] (i.e., the F4 site was placed on the C_4 symmetry axis that runs through the Sn atom in the *c*-direction). Second moments for the homonuclear and heteronuclear dipolar couplings, ($M_{2(II)}$ and $M_{2(IS)}$) of 9.4×10^7 and 0.4×10^7 Hz^2, respectively, were calculated with this model. $M_{2(II)}$ was calculated for the F2 site, and the value obtained for the F4 site was very similar. A very short value for T_{IS} of 140 ms is calculated with these values, with eq 4.

Model II. A much smaller value of $M_{2(IS)}$ of 1.95×10^5 Hz^2 was calculated by now only including all the fluoride ions in the Ba−Ba layer within a sphere of 8 Å radius from a central Sn^{2+} atom. Similarly, $M_{2(II)}$ was calculated by including all the couplings due to spin pairs within an 8 Å radius from a central fluorine spin in the Ba−Ba layer, yielding a value of 2.7×10^7 Hz^2. These values were used to calculate a much longer cross-relaxation time, T_{IS}, of 15.9 ms.

The value for T_{IS} obtained from model I is clearly much too short to account for the room-temperature CP process. This conclusion is consistent with our $T_{1\rho}$ measurements: because two very different $T_{1\rho}$ values are measured for the mobile and rigid spins, the ^{19}F spins cannot comprise a single thermodynamic spin bath. The value of T_{IS} obtained from model II is, however, in surprisingly good agreement with the experimental data, consistent with our original suggestion that the CP process involves the Ba−Ba fluorines only. Clearly, the motion in the Ba−Sn layer is sufficiently fast to remove the homonuclear and heteronuclear dipolar couplings involving spins in this layer, so that the Ba−Sn layer fluoride ions do not contribute to the polarization transfer process. The CP dynamics curve was calculated by using the calculated value of T_{IS} and the experimentally determined value for the $T_{1\rho}$ for the Ba−Ba spins, and the result is plotted in Figure 7. A reasonable agreement is obtained, given the limits of the model and the fact that we have not included the $T_{1\rho}$'s of the ^{119}Sn spins in the analysis.

The low-temperature data are not well described by model II, and it is clear that the fluorine atoms in the Ba−Sn (and Sn−Sn) layers must now start to contribute to the CP process. This is consistent with the similarity of the ^{19}F $T_{1\rho}$ values at low temperatures, which suggests that the ^{19}F spins are more strongly coupled and are close to forming a single thermodynamic spin bath. Using the $T_{1\rho}$'s determined at −150 °C, and the value of T_{IS} obtained from model I, a maximum in the CP intensity is predicted to occur at approximately 400 μs, which is shorter than the experimentally observed maximum of between 1 and 2 ms. Thus, some residual motion of the fluorine spins in the Ba−Ba layers appears to remain, even at the lowest temperature studied.

^{19}F T_1 (and $T_{1\rho}$) Variable-Temperature Measurements. The spin−lattice relaxation (T_1) values were measured from room temperature to 250 °C (Figure 8a) to help analyze the 2D magnetization-exchange data presented in the next section and to provide additional insight into the fluoride ion motion. The

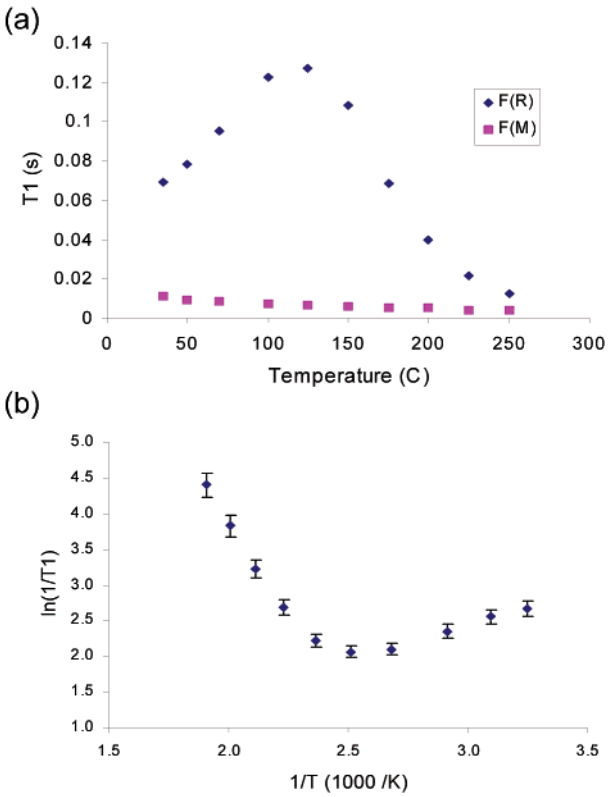

Figure 8. (a) Dependence of T_1 on temperature (35−250 °C) for the mobile and rigid fluorine sublattices, F_M and F_R. (b) Natural log of $1/T_1$ for the rigid sublattice (F_R) vs $1/T$ (temperature, T, in Kelvin).

mobile fluoride sublattice has an extremely short T_1 of 11 ms, while the ions in the Ba−Ba layer (the rigid sublattices) show a longer T_1 of 69 ms. On raising the temperature, the T_1's of the mobile sublattice decrease gradually, reaching a value of 4 ms at 250 °C. In contrast, the variation in the T_1's of the Ba−Ba fluoride ions is more complicated: First, the T_1's increase, reaching a maximum of 130 ms at approximately 125 °C. The T_1's then decrease rapidly, dropping to 12 ms at 250 °C. The plot of ln($1/T_1$) versus 1/temperature (Figure 8b) clearly shows that two T_1 regimes are present for the rigid (Ba−Ba) sublattice.

The $T_{1\rho}$ (data not shown) and T_1 values for the rigid sublattice are essentially identical from room temperature to 250 °C, indicating that the $T_{1\rho}$ values are controlled by the short T_1's of these spins in this temperature regime. The $T_{1\rho}$ values for the mobile sublattice remain very short (0.25−1.2 ms) up to 250 °C, and no clear minima or maxima are observed.

2D Magnetization Exchange.[33] Experiments were performed as a function of the mixing time to determine whether any exchange occurs between the two sublattices with slower exchange rates. Cross-peaks between the two fluoride ion sublattices start to become visible in the room-temperature 2D magnetization exchange spectra (Figure 9) at mixing times of 8 ms and above.

The intensities of both diagonal peaks decay as the mixing time increases, but the decay is much faster for the mobile fluoride ion peaks, in comparison to that for the rigid fluoride ions in the Ba−Ba layers. This unequal decrease in the peak intensities is attributed to the much shorter T_1 relaxation times of the mobile fluoride ions and will be discussed in more detail below. A cross-peak intensity ratio, $P_{A\rightarrow B}(t_{mix})$, can be calculated from the intensities of the diagonal (I_{AA}) and cross (I_{AB}) peaks

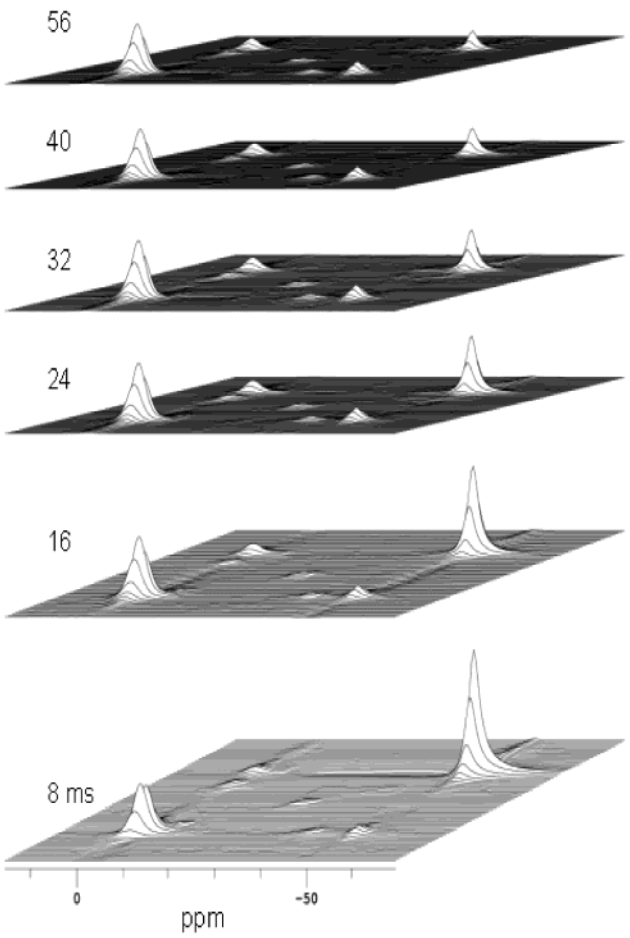

Figure 9. Room-temperature 2D magnetization exchange spectra for mixing times between 8 and 56 ms and a spinning speed of 12 kHz. The relative intensities are scaled to the intensity of the −3 ppm resonance.

using the following formula:

$$P = \frac{(I_{AA} - I_{AB})}{(I_{AA} + I_{AB})} \qquad (6)$$

The dramatically different relaxation times of the two sublattices means that the cross-peak intensities cannot be readily analyzed by using standard and widely used formulas, given in the literature.[33] (See for example, the 2D magnetization exchange study of lithium ion motion in a crystalline lithium silicate.[34]) In particular, unlike the case for a process involving a single T_1 relaxation time, the value of P_{AB} is no longer independent of the T_1 times of the fluorine ions. Thus, a plot of P vs t_{mix} will not necessarily follow a single-exponential curve of the form e^{-2kt} expected for a single rate process; this is clearly the case for the room-temperature data presented in Figure 10. The cross-peak ratio arising from magnetization transfer from the Ba−Sn/Sn−Sn fluoride ions (F_M) to the ions in the Ba−Ba layers (F_R) increases steadily as the magnetization time increases (Figure 10a). In contrast, the cross-peak ratio for transfer in the opposite direction appears to drop rapidly and then levels off at approximately 0.6, deviating significantly from the behavior

(33) Jeener, J.; Meier, B. H.; Bachmann, P.; Ernst, R. R. *J. Chem. Phys.* **1979**, *71*, 4546.
(34) Xu, A.; Stebbins, J. F. *Science* **1995**, *270*, 1332.

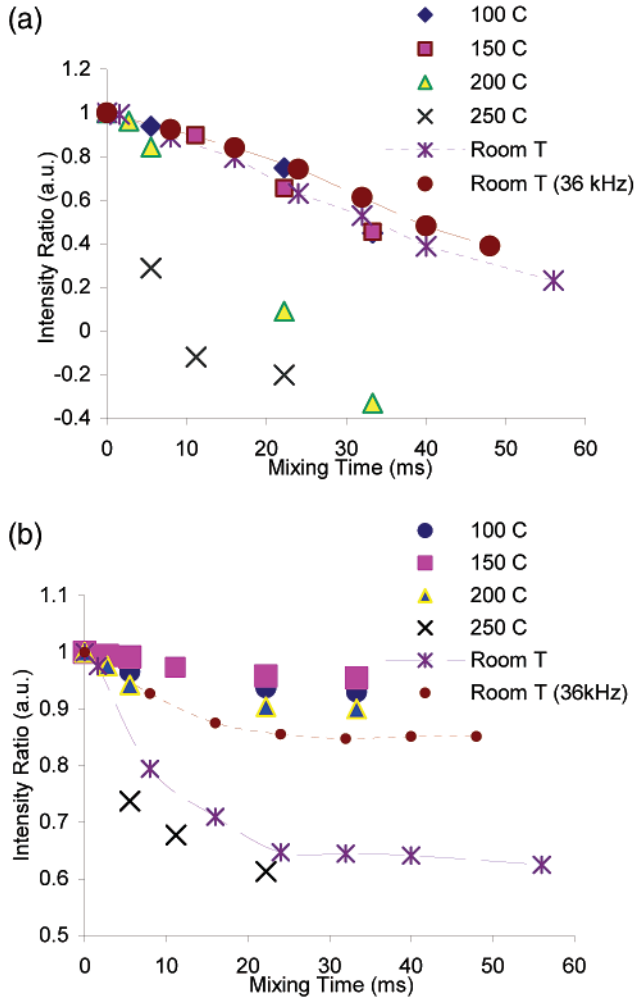

Figure 10. Plot of the 2D magnetization exchange cross-peak intensity ratio, P, versus mixing time for transfer from (a) the mobile fluoride ions, F_M, to the rigid ions, F_R, in the Ba−Ba layers ($P_{M\rightarrow R}$) and (b) F_R to F_M ($P_{R\rightarrow M}$). Two MAS spinning speeds were used: the data were acquired at a spinning speed of 12 kHz at room temperature, 100, 150, 200, and 250 °C, and also at a faster spinning speed of 36 kHz at room temperature.

Scheme 1

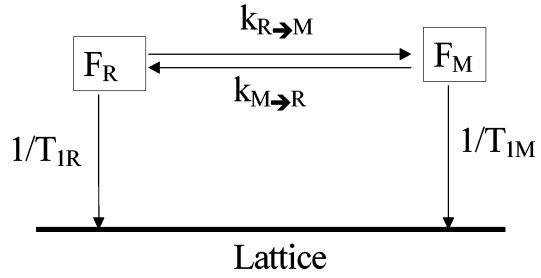

expected for a single rate process (Figure 10b). Very different apparent rates are required to fit the two sets of curves.

At least four rate processes are involved in controlling the magnetization exchange curves: $1/T_{1R}$, $1/T_{1M}$, $k_{R\rightarrow M}$, and $k_{M\rightarrow R}$, where T_{1R} and T_{1M} are 69 and 11 ms, respectively, the subscripts referring to the rigid (R) and mobile (M) sublattices (Scheme 1). Given the fixed concentration of ions in the two sublattices (1:3 for F_R:F_M), k_{R-M} and k_{M-R} are not independent, and $k_{R-M} = 3k_{M-R}$. Magnetization exchange from F_R to F_M, during the mixing time of the 2D experiment, creates F_M magnetization that decays much more rapidly than the F_R magnetization. Equilibrium will be established when $k_{R-R}[F_R] - k_{M-R}[F_M]$ is

of the same order of magnitude as T_{1M}. Under these conditions, new magnetization is transferred to the F_M sites as rapidly as it decays via a T_1 process. In contrast, magnetization exchange from F_M to F_R (the Ba−Ba fluorine spins) results in the creation of magnetization that becomes part of a pool of rigid fluoride ions with much longer T_1's (69 ms); the magnetization will, therefore, decay much more slowly. Hence, the cross-peak intensity, $P_{M\rightarrow R}$, grows steadily until at least 56 ms and is not expected to reach equilibrium and level off until longer mixing times. Thus, it is not surprising that the behavior of the two sets of spins is so different.

The two most common mechanisms for magnetization transfer between two sets of spins are spin-diffusion and chemical exchange. The former process, which is driven by the dipolar coupling and involves mutual spin flips between coupled spins, is normally reduced significantly in solids by fast MAS. Additional 2D magnetization exchange experiments were, therefore, performed with a probe capable of very fast MAS spinning to suppress any residual spin-diffusion between fluorine spins. The data collected at a MAS frequency of 36 kHz still show qualitatively similar cross-peak intensity ratios (Figure 10), but now the cross-peak ratio for spins originating in the Ba−Ba layers levels off at an even higher ratio (approximately 0.87). One likely explanation for this behavior arises from the difference in sample temperature, and thus T_1's, caused by the different MAS speeds and probes used to acquire the two sets of data. The sample temperature under fast MAS conditions is expected to be approximately 50 °C higher than the sample temperature under relatively slow MAS conditions. The higher temperature results in a longer T_1 for the F_R spins, but a shorter T_1 for the F_M spins; this is predicted to result in a leveling off of $P_{R->M}$ at a higher value, consistent with the experimental results.

2D magnetization-exchange experiments were performed at 100, 150, 200 and 250 °C, to explore the effect of temperature on the magnetization exchange process in more detail (Figure 10). Surprisingly, on increasing the temperature to 100 and 150 °C, $P_{R->M}$ decreases more slowly with mixing time than at room temperature. The results are similar to those obtained with fast MAS at room temperature, $P_{R->M}$ leveling off at approximately 0.93 and 0.95 at 100 and 150 °C, respectively. This apparent decrease in k_{R-M} appears to be consistent with an increase in T_{1R} and a decrease in T_{1M} as the temperature is increased. As the temperature is raised above 200 °C, k_{R-M} now appears to increase, $P_{R->M}$ dropping significantly as a function of the mixing time, decreasing more rapidly than the decrease observed at room temperature. Similarly, $P_{M->R}$ drops noticeably at 200 °C and above, becoming negative at mixing times of longer than 10 ms at 250 °C. A negative value of P indicates that the cross-peak intensity is larger than the intensity of the diagonal peak. The temperature dependence of P_{M-R} is consistent with an increase in $k_{M->R}$ at above 150 °C. The temperature dependence of these 2D spectra is clearly very complex, and will be discussed in more detail in the following section.

Discussion

The ^{19}F NMR data clearly provide experimental evidence for two different sublattices with very different dynamics. In contrast to previous wide-line studies, the MAS experiments allow the chemical shifts for the different fluorine sites to be determined, allowing assignments of the different sublattices, to the different sites in the crystal structure, to be made. The chemical shift, T_1, $T_{1\rho}$ values and the line width of the resonance observed at −3 ppm at room temperature, are consistent with its assignment to the rigid fluoride ions in the Ba−Ba layer. The second resonance is due to the mobile ions of the Ba−Sn and Sn−Sn layers. The coalescence of the resonances due to ions in this sublattice at temperatures of −100 °C and above indicates that the correlation time for the jump processes is approximately 3×10^{-5}s. The absence of any effects due to ^{19}F homonuclear and $^{19}F/^{119}Sn$ heteronuclear dipolar couplings involving these spins at room temperature is consistent with this correlation time for motion. The ^{19}F to ^{119}Sn CP experiments confirm the assignments of the resonances and the calculations of the CP dynamics clearly demonstrate that polarization transfer only occurs from the more distant spins in the rigid Ba−Ba layers at room temperature. At low temperature, the mobile spins start to freeze out on the time scale governed by the ^{19}F homonuclear coupling, which should be determined by $(M_{2(II)})^{-1/2}$ (i.e., $\approx 1 \times 10^{-4}$s) and the ^{19}F chemical shift. Even at the lowest temperature investigated (−150 °C), the cross polarization rate did not reach the value predicated for the rigid lattice, indicating some residual motion of the Ba−Sn/Sn−Sn fluoride ions. The high temperature ^{19}F MAS NMR spectra are consistent with additional exchange between different sites and/or a change in the sites that are occupied by fluorine.

The short T_1 and $T_{1\rho}$ relaxation times observed in these materials are attributed to field fluctuations due to motion. Both the T_1's and $T_{1\rho}$s of the two sublattices show complex behavior, which are clearly indicative of more than one set of dynamical processes. Motion is expected to reduce the T_1 substantially, when it enters the time scale governed by the Larmor frequency. For a dipolar-coupling driven relaxation process, the value of the T_1, and the T_1 minimum depends on the size of the dipolar coupling (or $M_{2(II)}$) via the following expression:[30]

$$\frac{1}{T_1} = \frac{6}{5}\frac{1}{M_{2(II)}}\left[\frac{\tau_c}{1 + w_0^2\tau_c^2} + \frac{4\tau_c}{1 + 4\omega_0^2\tau_c^2}\right] \qquad (7)$$

where ω_0 is the Larmor frequency. A similar expression can be written for $T_{1\rho}$, except ω_0 should be replaced by the rf field strength ω_1. A T_1 minimum occurs when $\omega\tau_C \sim 0.6$ and a significant reduction in the T_1 is not observed until $1/\tau_C$ approaches ω_0. The very short T_1's measured at room temperature and above suggest that the motion in this temperature regime is fast and must be close to $1/\omega_o$, even at room temperature; i.e., τ_c approaches 10^{-8} s. This very short correlation time is consistent with those already uncovered using other NMR techniques.

The observed T_1's for the mobile spins are shorter than predicted by the dipolar-mechanism alone, and thus must be affected by a combination of different relaxation mechanisms. One additional relaxation source come from the large ^{19}F chemical shift separations between sites, and the ^{19}F CSA of the different sites. The large numbers of different sites in the Ba−Sn and Sn−Sn layers, all with different chemical shifts, CSAs and presumably different correlation times, is consistent with the lack of a clear T_1 minimum for the mobile ions, and the weak dependence of the T_1 on temperature in the range investigated here. An additional source of the short T_1's may

also arise from any paramagnetic ions in the material. Since no clear T_1 minima are observed for either the rigid or mobile ions, it is difficult to obtain extract accurate values for the activation energies from the measured T_1 values. Nonetheless, the T_1 measurements are key to the interpretation of the 2D exchange data (see below) and confirm that the motion of the mobile ions approaches that typically observed for a liquid, even at room temperature.

There are at least two possible sources for the relatively short T_1's and $T_{1\rho}$s of the "rigid" sublattice at room temperature and above. First, the very rapid motion of fluoride ions in the Ba−Sn fluoride ion sublattice can result in fluctuating fields that will reduce the T_1's of the Ba−Ba sublattice, via a dipolar-driven, cross-relaxation process between the two sublattices. This process is analogous to the mechanism that can result in a nuclear Overhauser effect in liquids.[35] Second, the onset of jump processes (i.e., chemical exchange) between the two sublattices should also result in a gradual reduction of the Ba−Ba T_1 time, so that it approaches that of the mobile ions. The first process occurs for correlation times for motion close to the Larmor frequency, which is consistent with the values of τ_C estimated directly from the T_1's of the mobile sublattice. Thus, we ascribe the reduction of the T_1 of the rigid ions, observed near room temperature to this cross-relaxation process. Furthermore, the increase in the T_1 as the temperature is increased, suggests that we are above the T_1 minimum caused by this mechanism (i.e., $\tau_c < 0.6/\omega_0$). The T_1 decrease above 150 °C can then be ascribed to increased *chemical* exchange between the two sublattices. This mechanism will become gradually more important as the temperature increases, and appears to dominate above 150 °C.

The short $T_{1\rho}$s (for both sets of ions) in this temperature regime are largely a consequence of the short T_1's in this temperature regime, and do not necessarily provide additional information. A more detailed investigation of the T_1's and $T_{1\rho}$s over a wider range of temperatures and magnetic field strengths is now in progress, to attempt to separate some of these different processes.

The 2D magnetization exchange data provide an important check on our proposals for the source of the relaxation mechanisms for the rigid ions. The two most important magnetization transfer mechanisms that typically result in cross-peak intensities are (i) the spin-diffusion "flip-flop"-type exchange driven by the dipolar interactions between the two spin reservoirs and (ii) the chemical exchange or actual jumps of the fluoride ions in and out of the Ba−Ba layers into the Ba−Sn layers. The rapid motion of the mobile fluoride ions is expected to reduce the dipolar coupling between the two sublattices significantly, and MAS should readily remove any residual dipolar coupling. Furthermore, the large chemical shift separation between the sublattices will also help quench this spin-diffusion process. For example, measurements for the oxyfluoride $Ba_2WO_3F_4$, which contained two sets of resonances separated by approximately 75 ppm showed spin-diffusion rates of 2.6 s^{-1} (i.e., $\tau_C = 400$ ms) at a spinning speed of 18 kHz. A substantial contribution to the exchange process via the typical spin-diffusion process seen in rigid solids can be further excluded on the basis of the following experimental observations: First, the line shape and line widths of the resonance due to the mobile ions and absence of spinning sidebands are not consistent with strong dipolar coupling between the mobile spins, or between the two sublattices. Second, the 2D line widths of the F_M diagonal and cross-peaks are Lorentzian, which again is not consistent with any dipolar coupling between the spins. In apparent contradiction with this, the 2D magnetization exchange data indicate that significant exchange does occur between the two sublattices on the time scale probed by the longer mixing times used in the 2D experiments (i.e., approximately 10−40 ms) at room temperature. Furthermore, the apparent exchange rate appears to decrease as the temperature is increased and then increases significantly at 200 °C and above. This is not consistent with a simple chemical exchange process. Thus, we propose that spin-diffusion (or cross-relaxation), driven by the same process that was responsible for the short T_1's of the rigid sublattice, results in the magnetization exchange observed between the two sublattices at room temperature. As the temperature increases, this process gradually decreases, resulting in a reduction in k_{R-M} and k_{M-R}. The increase in the exchange rate at 200 °C is then ascribed to the onset of actual magnetization exchange between the sublattices, which will increase as the temperature is raised. Thus, at 250 °C, exchange between the two sublattices is clearly occurring on the time scale governed by the mixing time of the 2D exchange experiment.

Scheme 2

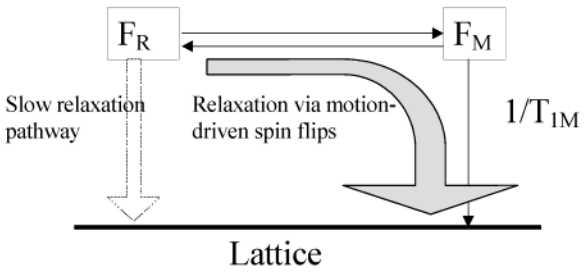

The 2D results, in combination with the T_1 measurements, indicate that the major T_1 relaxation pathway for the rigid spins at room temperature and above occurs via the mobile spins; the T_1 pathway directly to the lattice, shown earlier in Scheme 1, appears to be associated with a much larger T_1 value and is not a major relaxation pathway. The dominant relaxation pathways, based on the experimental data, are shown in Scheme 2. Thus, $k_{R\rightarrow M}$ represents the rate-limiting step in the T_1 mechanism for the F_R spins. Furthermore, since $T_{1M} \ll T_{1R}$, $k_{R-M} \approx 1/T_{1R}$. An estimate for k_{R-M} may then be obtained on the basis of Scheme 2 and the T_{1R} data presented in Figure 8. For example, $1/k_{R\rightarrow M} \approx 10^{-2}$ s at 250 °C. This is consistent with the data presented in Figure 10. A detailed analysis of 2D magnetization exchange curves is in progress, and the results will be reported elsewhere.

Implications for the Conduction Mechanism of $BaSnF_4$. Rapid motion occurs primarily in the Ba−Sn sublattices at ambient temperature. Even at room temperature, the T_1 times are very short, indicating that motion in the Ba−Sn/Sn−Sn layers is occurring even on the much faster time scale probed by this measurement (τ_C approaches $\sim 10^{-8}$ s). This very short correlation time is consistent with the value for τ_c estimated at −100 °C ($< 3 \times 10^{-5}$ s^{-1}) and the activation energy for motion of 0.34 eV measured by Denes et al.[14] for $BaSnF_4$ in this temperature regime. Chadwick et al.[15] measured an activation

(35) Ernst, R. R.; Bodenhausen, G.; Wokaun, A. *Principles of NMR in one and two dimensions*; Clarendon Press: Oxford, 1987.

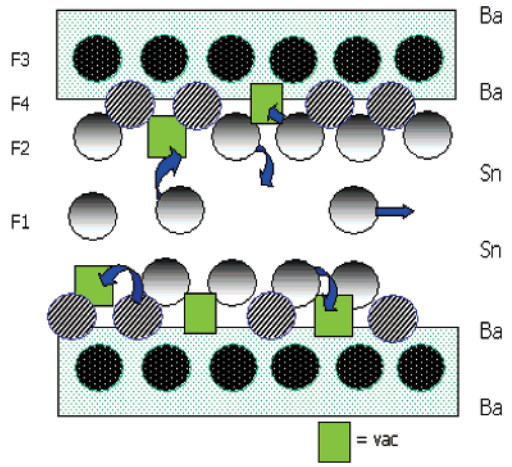

Figure 11. Diagram illustrating some of the major conduction pathways in $BaSnF_4$ (view down the [100] direction). The rigid Ba−Ba layers prevent rapid conduction in all three directions. The vacancies in the partially occupied Sn−Sn layers are omitted for clarity.

energy of 0.5 eV, and on the basis of these two activation energies, the correlation time is expected to decrease by a factor of between 6×10^3 (0.34 eV) and 3×10^5 (0.5 eV) between 173 and 273 K. Thus, the activation energy measured by Chadwick et al. is higher than the activation energy suggested by our NMR results. Chadwick et al. observed a discontinuity in σ just below 0 °C and an activation energy of 0.18 eV above this temperature. In contrast, Denes et al. observed a discontinuity in σ at 127 °C, and the activation energy dropped slightly to 0.31 eV above this temperature. The differences between the two sets of measurements presumably results from small differences in sample stoichiometry, impurity level, or sample preparation method.

The magnetization exchange experiments demonstrate that slow exchange between the two sublattices does occur, but with a correlation time that is at least 6 orders of magnitude slower than the motion in the mobile layer; i.e. slow jumps between Ba−Sn and Ba−Ba layers occur on the 10 ms time scale at 200 °C and above. This is an important observation, because this exchange process is required for three-dimensional conductivity.

A model for the conductivity is shown in Figure 11. The Ba−Sn layers clearly contain large concentrations of filled and vacant interstitial sites, allowing rapid conduction in this layer and jumps from the fully filled Ba−Ba layer to occur. The disorder in this layer is consistent with the relatively low activation energy for the jump processes near room temperature. The high conductivity is consistent with the large number of mobile ions. Given the large numbers of vacant sites in the Ba−Sn layers, it appears extremely likely that the major mechanism for motion of the Ba−Ba ions involves interlayer jumps between the mobile and rigid layers, rather than a direct intralayer F3-to-F3 jump. This intralayer jump process requires a vacancy on the F4 sublattice, and these vacancies should be present in significant concentrations in this highly disordered system.

The results for $BaSnF_4$ should be contrasted with the ^{19}F MAS NMR results for $PbSnF_4$ presented in our earlier communication.[21] Motion in $PbSnF_4$ was seen to involve all the fluoride ions on the NMR chemical shift time scale, at ambient temperatures. Furthermore, unlike $BaSnF_4$, the ionic motion in $PbSnF_4$ is sufficient to remove the ^{19}F homonuclear dipolar coupling between all the spins, even at room temperature, and two distinct sublattices are not so clearly observed by NMR. Thus, it appears likely that the more polarizable Pb^{2+} ion appears to play an important role in improving conduction in the *c*-direction. Distinct fluorine ion sites are not clearly resolved by NMR for $PbSnF_4$, consistent with the neutron diffraction results, where a better refinement of the structure was obtained for $BaSnF_4$ in comparison to $PbSnF_4$.

Conclusion

Solid-state NMR has been used to develop a detailed understanding of the anionic conduction in $BaSnF_4$. ^{19}F MAS NMR spectroscopy was used to identify the sublattices responsible for conduction. CP experiments were used to help confirm the assignments of the resonances and to probe mobility: Transfer of polarization to Sn occurs over a distance of 4.7 Å from the distant fluorine spins in the Ba−Ba layers. The fluorine ions near Sn are mobile at room temperature and do not appear to contribute significantly to the CP intensity. Consistent with this suggestion, calculations of the CP transfer rate, based on a model that assumes that the Ba−Ba fluorides are primarily responsible for the CP processes, are able to predict, with surprisingly good agreement, the experimentally observed value for T_{IS}. The "mobile" fluoride ions slow down as the temperature is reduced, and by −150 °C they are essentially rigid on the NMR time scale. Three new local environments are identified which are assigned to different fluoride ions in the Sn−Ba and Sn−Sn layers. The variable-temperature ^{19}F NMR data indicate that the jump frequencies for these fluoride ions are greater than 15 kHz, even at −100 °C. By using a combination of 2D magnetization exchange experiments and T_1 measurements, we were able to probe correlation times varying over 6 orders of magnitude. The 2D experiments probe slower motion ($\tau_c = 10^{-2}$ s) and showed that the fluoride ions in the BaF_2 layers start to exchange with the mobile ions at 200 °C and above. The T_1 measurements illustrate that the correlation times for the mobile ions are extremely short in the same temperature regime ($\tau_c = 10^{-8}$ s at room temperature). Furthermore, this rapid motion results in a dipolar-driven cross-relaxation process, which is driven by fluctuating fields of the mobile ions and reduces the T_1's of the rigid ions significantly. This behavior is more typically seen in liquid-state than in solid-state NMR.

Our study has revealed a series of NMR phenomena that occur in the presence of rapid motion *and* high magnetic field strengths. Unlike wideline NMR relaxation studies of fluorides, which were typically performed at much lower fields, chemical shift and CSA effects now become a major relaxation mechanism; this source of relaxation appears to be larger than that due to dipolar relaxation and, hence, cannot be ignored in the analysis of the relaxation time data. T_1 (and $T_{1\rho}$) values are so short in this system that they can result in extremely inefficient cross-polarization processes involving these spins. However, in the example shown in this paper, we actually exploited the short $T_{1\rho}$'s of the mobile sublattices to obtain CP curves for transfer from the other (rigid) sublattice. The short T_1's also resulted in 2D magnetization data that could not be rationalized by

modeling the data with a single rate process. Further experiments are currently in progress to explore these phenomena at different field strengths in order to extract more detailed information concerning the motion in this system.

Acknowledgment. The authors acknowledge funding from NSF (DMR0074858 and DMR9901308) and NATO Grant CRG972228. The authors thank Paul Madden, Michael Castiglione, and Mark Wilson for stimulating discussions, Steve Hull for his help with the neutron diffraction experiments, and Wiebren Veeman for discussions concerning the analysis of NMR data.

Supporting Information Available: $BaSnF_4$ ^{19}F spectra at -150 °C: A comparison of the one pulse and echo spectra (Figure S1) and intensities of the resonances at -3, -47, and -74 ppm as a function of spin-locking time (Figure S2) (PDF). This material is available free of charge via the Internet at http://pubs.acs.org.

JA026155J